Available online at www.sciencedirect.com
SCIENCE DIRECT
Carbohydrate Polymers 59 (2005) 27–35
Carbohydrate Polymers
www.elsevier.com/locate/carbpol

Analysis of calcium salt of carboxymethyl cellulose: size distributions of parent carboxymethyl cellulose by size-exclusion chromatography with dual light-scattering and refractometric detection

Bedřich Porsch[a,*], Bengt Wittgren[b]

[a]*Department of Supramolecular Chemistry, Institute of Macromolecular Chemistry, Academy of Sciences of the Czech Republic, Heyrovsky sq. 2, 162 06 Prague 6, Czech Republic*
[b]*AstraZeneca R&D Mölndal, SE-431 83 Mölndal, Sweden*

Received 2 March 2004; revised 9 July 2004; accepted 20 August 2004
Available online 27 September 2004

Abstract

Generally, the insoluble calcium salt of carboxymethyl cellulose can be quantitatively transformed in a batch process into its sodium form using chelating resin Lewatit TP-208. The resulting sodium carboxymethyl cellulose, having a fairly low degree of substitution close to 0.6, was analysed using size exclusion chromatography with multiangle light scattering/refractometric detection. Commercial samples of sodium carboxymethyl cellulose having degree of substitution 0.7 and 1.2 were used to highlight the relation between the degree of substitution and the presence of aggregated structures. It was found that all calcium/sodium transformed carboxymethyl cellulose samples contain a significant amount of macrogel particles larger than 5 μm which can be removed by centrifugation or filtration. Centrifuged and filtered samples were then shown to contain significant amounts of smaller aggregated structures (fringed micelles) which were found also in sodium carboxymethyl cellulose reference samples where their amount was inversely proportional to their degree of substitution. Because size exclusion chromatography separates macromolecules according to their hydrodynamic volume, linear and aggregated structures having the same hydrodynamic volume, but entirely different molar mass, are eluted together and a significant heterogeneity in terms of molar mass at a fixed elution volume is found especially at lower sample elution volumes. Hence, molar mass distributions become undefined. Fortunately, the elution was found to be homogeneous in terms of experimentally accessible radii of gyration and reliable size distributions could be evaluated.

Keywords: Calcium carboxymethyl cellulose; Sodium carboxymethyl cellulose; Size exclusion chromatography; Dual RI-MALS detection; Size distribution

1. Introduction

Calcium salt of carboxymethyl cellulose (CaCMC) finds the main use in tablet formulations where it is used as a binder, diluent and disintegrant. Although CaCMC is insoluble in water, it is an efficient disintegrant because it swells to several times of its original volume on contact with water (Wade & Weller, 1994). Commercial products are mostly characterized only by some particle size of dry product and pH value of their aqueous dispersion. Being insoluble in any solvent, direct characterization of CaCMC in terms of molecular weight and size is impossible and can be done only after its quantitative transformation to some soluble form, preferably sodium salt. More detailed knowledge of their composition like calcium content and molar mass as well as particle size of parent sodium carboxymethyl cellulose is desirable in pharmaceutical industry because there is a close relation between these parameters and the CaCMC tablet technology/application performance. The preferred CaCMC disintegrant should have a high molar mass, together with a low average degree of substitution (DS); typical DS of CaCMC was reported to be 0.6 ± 0.1 (Doelker, 1993). There is a danger of its incomplete solubility in water even if such a CaCMC

* Corresponding author. Tel.: +420 296 809 350; fax: +420 296 809 410.
E-mail address: porsch@imc.cas.cz (B. Porsch).

0144-8617/$ - see front matter © 2004 Elsevier Ltd. All rights reserved.
doi:10.1016/j.carbpol.2004.08.019

derivative is transformed to its sodium form (NaCMC) because a minimum DS which guarantees complete water solubility should be at least 0.7 (Just & Majewicz, 1985). Highly swollen but insoluble gel particles/aggregates then appear in solutions of the samples having DS below 0.7 and their amount increases with decreasing DS.

Ion-exchange is a natural choice when CaCMC should be transformed to the sodium form. This requires to perform ion-exchange in the batch mode because of CaCMC insolubility in any solvent. Fortunately, chelating ion-exchange resins should have sufficient selectivity to accomplish quantitative Ca/Na exchange in a batch experiment. (Samuelson, 1963). Having CaCMC transformed to the soluble form, size exclusion chromatography may be used to characterize its molar masses and dimensions. The use of dual light scattering/refractometric detection appears to be a must here because the low degree of substitution predetermines the presence of both macrogel and microgel particles (Just & Majewicz, 1985) together with polymer coils formed from linear chains in the transformed samples. Such particle system is characterized by a variable mass/hydrodynamic volume ratio of the various particles present, which means that both molar mass and size information are needed to interpret SEC separation experiments where separation is governed by a hydrodynamic volume of the analyzed particles preferably expressed by its cube root (Potschka, 1987, 1988, 1991) in terms of a radius R_{SEC}. In the case of SEC of polyelectrolytes using packings of the same charge, both the effective hydrodynamic volume of a solute and the interfacial pore wall effect must be accounted for. In general, separation is governed by some overall radius R

$$R = R_{SEC} + R_{IF} = R_{SEC} + \kappa^{-1}\bar{a} \quad (1)$$

where $\bar{a}$ is the average electrostatic repulsion distance at equilibrium in multiples of Debye length κ^{-1}, R_{SEC} is the rotationally averaged mean radius of the solute and R_{IF} is the interfacial contribution to the total solute radius R. Actually, R_{IF} is introduced to account for the reduced pore size under low-salt conditions. For spherical particles like proteins, R_{SEC} should be simply the sphere radius but for the case of the coiled polyelectrolyte, it can be a complex function of ionic strength. The generally accepted universal calibration approach predicting congruent polymer elution irrespective of their composition and architecture then assumes negligible R_{IF}, i.e. high ionic strength conditions, and

$$R_{SEC} \sim \{[\eta]M\}^{1/3} \quad (2)$$

where $[\eta]$ is the intrinsic viscosity and M is the molar mass of a macromolecule in bulk solution. The Flory–Fox theory (Flory & Fox, 1951) predicts that

$$[\eta]M = \Phi[\langle r_g^2\rangle^{1/2}]^3 \quad (3)$$

where $\langle r_g^2\rangle^{1/2}$, mostly abbreviated as r_g, is the root mean square radius (commonly denoted radius of gyration) of a macromolecule and Φ should be a universal proportionality constant originally assumed to be valid for flexible uncharged polymers soluble in organic solvents if their molar mass exceeds a minimum value around 50 000. Assuming validity of Eq. (3), R_{SEC} should be proportional to r_g as another universal calibration parameter. Nevertheless, the universality of r_g must be always verified experimentally before use, because it is highly questioned especially for semirigid polymers soluble in aqueous solvents, mostly due to observed variations of the Φ value with their architecture and/or molar mass (Ioan, Aberle, & Burchard, 2001; Radke, 2001)

It will be shown in this paper that CaCMC can be quantitatively transformed into its sodium salt form, which makes possible SEC analysis. NaCMC polymers having variable DS will be used as model systems and compared to transformed CaCMC samples. An evidence of the presence of both macrogels and fringed micelles in the transformed samples will be presented. Guidelines how to interpret molar mass and size data when the samples contain linear macromolecules and non-negligible mass amounts of aggregates of the same hydrodynamic volume will be described and the impact of their low DS on the data will be evaluated.

2. Experimental

2.1. Materials

CaCMC samples were commercial products of Nichirin Chemical Industries Ltd (Hyogo, Japan). Four different batches coded as A, B, C, and D were analyzed. Two NaCMC model samples having nominal molar mass 250 000 and DS 0.7 and 1.2 were supplied by Sigma-Aldrich (Stockholm, Sweden). Chelating resin Lewatit TP-208 was obtained from Fluka (Buchs, Switzerland). Analytical reagent grade NaCl was obtained from Merck (Darmstadt, Germany) and used without further purification. Water was from a Millipore Milli-Q^{UF}_{PLUS} ultrapure water purification unit (Millipore Corp., Bedford, MA, USA).

2.2. Chromatography

The modular chromatograph consisted of a Degasser X-act (Your Research, Onsala, Sweden), a Constametric® 3200 MS pump (Thermo Separation Products, Riviera Beach, FL), a V-451 PEEK six port injection valve with 100 μl loop (Upchurch Scientific, Oak Harbor, WA, USA), a DAWN-DSP multi-angle light scattering photometer (Wyatt Technology, Santa Barbara, CA, USA). Simultaneous concentration detection was performed using an R-401 differential refractometer (Waters Assoc., Milford, MA, USA). Filtered toluene (Merck, Darmstadt, Germany) was employed for calibration of the MALS detector and

sodium chloride for calibration of the refractive index detector. The detectors at different angles in the MALS instrument were normalized to the 90° detector using a narrow pullulan standard P-50 (Shodex standard P-82, Showa Denko, Tokyo, Japan). The signals from the two detectors were analysed by ASTRA software (ASTRA for Windows 4.50) (Wyatt Technology, Santa Barbara, CA, USA). The angular dependence of the scattered light was extrapolated to zero angle using the linear Berry fit method to obtain molar mass and radius of gyration as a function of elution volume. The effect of the second virial coefficient may be neglected because of very low concentration of eluted species in a SEC experiment. Refractive index increment (Picton, Merle, & Muller, 1996) $dn/dc = 0.147$ ml/g was used in the calculations. The recovery was obtained from the ratio of the mass eluted from the column (determined by integration of the refractometer signal) to the mass injected. The mobile phase was always an 0.1 M sodium chloride solution which was 3 mM in sodium azide.

A set of three columns (8×250 mm) in series packed with hydrophilized GMB 200, 1000, 5000+poly(glycidyl methacrylate) packings (Labio, Prague, Czech Republic), particle size 10 μm, having for poly(ethylene oxide) a linear calibration in terms of log M vs. elution volume from 2×10^4 extended above 5×10^6, was used for centrifuged as well as filtered samples. A TSK-GEL column GMPW 5000, 7.8×600 mm, particle size 17 μm, molar mass separation range 4000–1×10^6 for poly(ethylene oxide) was used for the analysis of filtered samples.

2.3. Ca/Na ion exchange

In a typical procedure, 20 mg of CaCMC was suspended in 20 ml water, 5 g of Lewatit TP-208 was added and the mixture was shaken overnight. A separate experiment with the same amount of ion-exchange resin in a dialysis bag was performed to verify that no adsorption of NaCMC takes place. The only observable difference was found as expected in much slower ion exchange; 3 days were needed in this case. The slightly hazy supernatant solutions of all four samples were then freeze-dried and no detectable content of Ca was found using Perkin Elmer Model 3110 atomic absorption spectrometer. The content of Ca in CaCMC samples was determined as well and used to calculate their DS values. The mass balance before and after the ion exchange with and without dialysis bag has shown that no loss of sample took place when the resin is in direct contact with a sample suspension.

2.4. Sample solutions

The supernatant solutions after Ca/Na exchange were diluted 1:1 with 0.2 M NaCl to adjust the NaCl content close to that of the mobile phase. Further dilutions (if necessary) were made with the mobile phase. The reference NaCMC samples were also dissolved in pure water and their ionic strength was adjusted to 0.1 M NaCl by 1:1 dilution with 0.2 M NaCl because in particular NaCMC having DS 0.7 dissolved in the mobile phase exhibited much worse filtration behavior (faster plugging) using the same filter when compared with its solution prepared in pure water with subsequent adjustment of ionic strength.

Sample filtrations prior to injections were performed using a Cole-Palmer 74900 syringe pump (Cole-Palmer, Vernon Hills, IL, USA) at a flow rate of 2 ml/h. Filters having porosity 5 μm (Millex-SW, Millipore, Bedford, MA, USA), 2 μm (Puradisc™ 25GD, Whatman, Maidstone, UK), 1 μm (Puradisc™ 13 mm, Whatman), 0.45 μm (HV_{13}, Millipore) and 0.22 μm (GV_{13}, Millipore) were used. Alternatively, the solutions were centrifuged for 3 h at 15 000 rpm on a preparative ultracentrifuge Beckman LB-55.

3. Results and discussion

The degree of substitution of all four CaCMC samples was calculated to be within the range 0.59–0.62 and they may be thus viewed as almost identical. An agreement with typical values of DS for CaCMC published by Doelker (1993) was found and these low DS values predetermine the incomplete molecular solubility of NaCMC obtained after the Ca/Na ion exchange. NaCMC solubility study (Dautzenberg, Lukanoff, & Hicke, 1990) has shown that only 75% of the laboratory-made NaCMC sample from cotton linters having average DS 0.63 dissolved in water. Industrial NaCMC samples of various origin with DS between 0.58 and 0.61 contained about 10–20% of highly swollen but water-insoluble aggregated particles. Hence, the presence of macrogel as well as microgel particles together with linear chains in NaCMC samples obtained after conversion of CaCMC to sodium form is unavoidable. The particles larger than 500 nm are usually called macrogels and the smaller microgels (Gruber, 1979; Just & Majewicz, 1985). Their structure seems now well established, microgels being termed fringed micelles (Schulz & Burchard, 1993; Schulz, Burchard, & Dönges, 1998, chap. 16; Schulz, Seger, & Burchard, 2000). Because of the expected complexity of SEC analysis of these slightly hazy samples, model NaCMC polymers of variable DS forming clear solutions in water were analyzed first as a possible simpler reference system.

The log M vs. elution volume calibrations obtained for 0.45 μm filtered and centrifuged NaCMC sample having DS = 0.7 are presented in Fig. 1. A strong upward curvature is immediately visible. The observed deviation is a clear manifestation of an increase in the mass/hydrodynamic volume ratio because the column set used separates according to hydrodynamic volume and is known to provide linear calibration in terms of log M vs. elution volume for

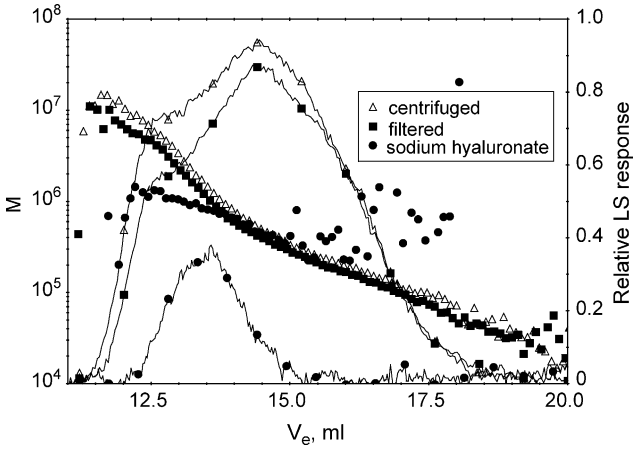

Fig. 1. Molar mass of 0.45 μm filtered and centrifuged NaCMC sample (DS = 0.7) and sodium hyaluronate as a function of elution volume (lines indicate corresponding LS signals at 90°).

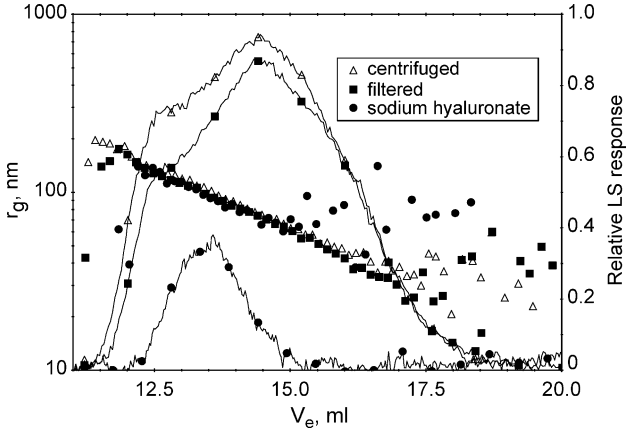

Fig. 2. Comparison of r_g vs. elution volume plots of 0.45 μm filtered and centrifuged NaCMC sample (DS = 0.7) and sodium hyaluronate.

a linear homopolymer. The log M vs. elution volume calibration for sodium hyaluronate, a linear semirigid polysaccharide carrying carboxylic groups, obtained under identical conditions (Fig. 1) illustrates the calibration linearity expected in this case. The detectable deviation from linearity begins around $M \sim 500\,000$ and indicates the onset of the presence of more dense fringed micelles. Their mass content seems to increase with increasing molar mass; on the other hand, the macromolecules having molar masses below 500 000 appear to be essentially linear. Also, there is an observable difference between filtered and centrifuged sample in Fig. 1. The filtration procedure should remove particles according to their size and formation of a 'filtration cake' must be expected after a certain volume is filtered. Low flow rates prevent the cake from being compressed and linear coiled macromolecules should be able to pass the filter. On the other hand, other structures should be gradually removed and finally the filter should be blocked. This behavior was observed with this sample when filtration was performed manually at flow rates estimated somewhere between 1 and 2 ml/min. The filter was blocked after filtration of ~0.5 ml. On the contrary, several millilitres of this solution could be filtered with the same filter at low speed 2 ml/h without any significant increase in pressure resistance. Centrifugation should, roughly speaking, remove particles according to their density and the secondary filter cake effect should be absent. An annoying result follows from Fig. 1; above molar mass about half a million, a high 'slice' heterogeneity in terms of molar mass must be assumed due to mixing of various structures having variable density but the same hydrodynamic volume. Hence, the calculation of molar mass distribution (MMD) becomes obscure.

Fig. 2 contains log r_g vs. elution volume plots for the same NaCMC and sodium hyaluronate samples as in Fig. 1. It is seen that r_g values of all three samples follow within the experimental error one straight line. The use of a linear column set is especially advantageous here; it is easy to show by a simple algebra that the universal calibration plot in terms of log([η]M) vs. elution volume should be linear as well if the Mark–Houwink equation applies.

The Flory–Fox theory then predicts in this case (Eq. (3)) that a plot of log r_g vs. elution volume should also be a linear one. Sodium hyaluronate was shown (Reed, 1995) to obey Eq. (3) even when ionic strength was varied, which means that its hydrodynamic volume is proportional to the cube of r_g and the use of r_g instead of R_{SEC} as a universal calibration parameter is possible here. Let us note that variable R_{IF} in Eq. (2) conveniently explains the observed shifts of sodium hyaluronate log r_g vs. elution volume plots when the ionic strength was varied (Reed, 1995). Hence, it follows from Fig. 2 that separation according to hydrodynamic volume can be described in terms of gyration radii in our case and 'slices' heterogeneous in M are homogeneous in r_g. In other words, the picture shows that this is a specific case where r_g can be used as a universal calibration parameter for both the fringed micelles and linear NaCMC chains. Therefore, size distributions in terms of r_g appear to be well defined here. This conclusion should not be generalized for other cellulose derivatives because recently studied hydroxypropyl cellulose (Wittgren & Porsch, 2002) is an example of a non-congruent elution in terms of r_g. Fig. 3 shows the difference between log M vs. V_e plots for filtered NaCMC samples having DS 0.7 and 1.2. A significant decrease in the number of fringed micelles in the more substituted sample is immediately visible. As shown in Fig. 4 for filtered samples, the congruent elution in terms of r_g persists for samples having different DS values.

Centrifugation of the more substituted sample does not remove small aggregated structures eluted between 15 and 17 ml (Fig. 5) which are partially removable by filtration as follows from Fig. 3. The deviation of RI traces obtained for centrifuged samples with DS 0.7 and 1.2 is displayed in Fig. 6. A fairly small but clearly detectable difference is observed as a shoulder at the low elution volume sides of peaks; otherwise peaks are almost identical and can be compared to LS signals presented in the background of

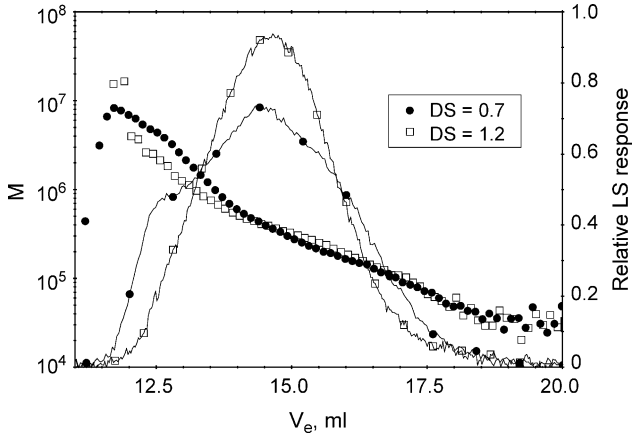

Fig. 3. Comparison of molar mass vs. elution volume plots of 0.45 μm filtered NaCMC samples having different degree of substitution.

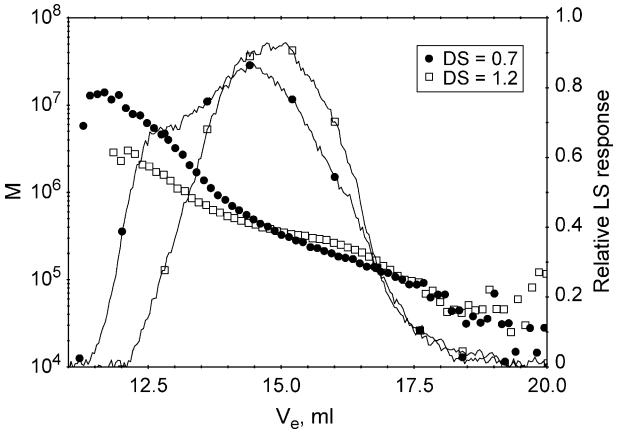

Fig. 5. Comparison of molar mass vs. elution volume plots of centrifuged NaCMC samples having different degree of substitution.

Figs. 1–5. Quite pronounced variations of LS intensity when compared to small changes of RI signal can be seen indicating that a rather small but detectable mass amount of fringed micelles is responsible for a pronounced increase in scattered intensity. This means that M_w in a slice is measured and a local polydispersity of that slice (in terms of M) may be very high for M values above 500 000. In other words, this part of the chromatograms reflects a mixture of a small mass amount of fringed micelles and linear coils having the same hydrodynamic volume and, fortunately, also experimental r_g value. The weight based differential distribution of r_g $G[r_g]$ is defined as a weight fraction of the sample having r_g in an interval r_g, $r_g + dr_g$ and the condition of a homogeneous size within a slice is satisfied. The corresponding correct weight based differential distribution of M giving weight fraction of molecules having M in an interval M, $M + dM$ cannot be calculated because a pronounced slice heterogeneity is found for elution volumes below 14 ml (Figs. 1, 3 and 4). It follows from Fig. 6 that this biased part of the sample represents only a minor part of the total sample mass but is clearly detectable at least for sample having DS = 0.7 on the mass scale. The only experimentally accessible function, which would describe 'distribution' of M_w values against the weight–average molar mass, does not conform with the definition of a distribution function. The only possibility would be to use a straight line fit of a linear part of log M vs. V_e calibration for the whole sample to calculate MMD of linear macromolecules (i.e. to neglect the presence of fringed micelles in terms of their molar mass). Such an approximation would be correct only having experimental evidence that the mass of fringed micelles in the sample is below the detection limit of RI (mass) detector which is in contradiction with the data in Fig. 6. This approach was used in our previous report (Wittgren & Porsch, 2002) dealing with the presence of fringed micelles in hydroxypropyl cellulose where such evidence was available but is hardly acceptable here. Therefore, only r_g distributions of the samples are compared in Fig. 7. Having the linear column behavior in terms of size, the distributions could be extended using linear fit below 20 nm where experimental r_g values are not directly accessible. The less substituted sample is found to be wider in terms of size. Generally valid

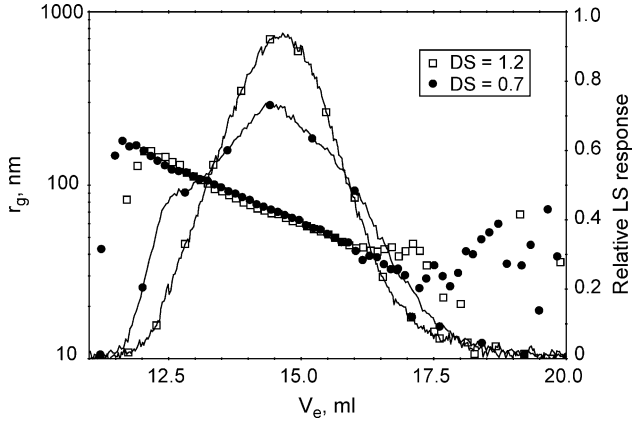

Fig. 4. Comparison of r_g vs. elution volume plots of 0.45 μm filtered NaCMC samples having different degree of substitution.

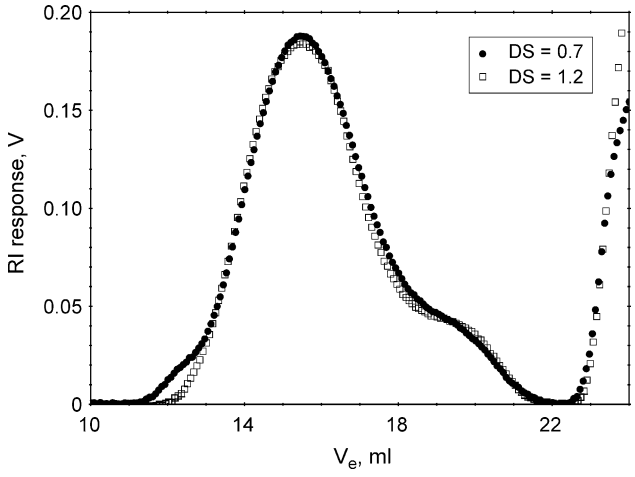

Fig. 6. Comparison of refractometric signals of centrifuged NaCMC samples having different degree of substitution.

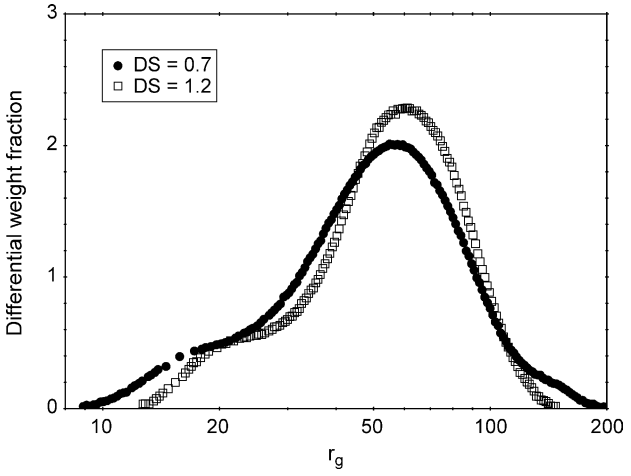

Fig. 7. Size distributions of NaCMC samples having different degree of substitution.

M_w values were calculated for DS 0.7 and 1.2 to be 586 000 and 360 000 and the corresponding z-average r_g values 118 and 82.7 nm, respectively. Higher value of molar mass and size average simply reflects the higher content of fringed micelles at lower degree of substitution. The usually calculated polydispersity index (the ratio of weight average to number average molar mass) M_w/M_n becomes only apparent here because the relation $c_i = n_i M_i$ (where n_i is the number of molecules of M_i) used in calculation of M_n (as well as the number distribution) is not applicable in the case of slice heterogeneity observed here.

The centrifuged Ca/Na transformed CaCMC samples exhibited qualitatively similar behavior. As shown in Fig. 8 for the batch D, the amount of fringed micelles increases significantly when compared with centrifuged sample of NaCMC. Also, it follows from this comparison that even centrifuged NaCMC sample having DS = 0.7 contains some small fringed micelles eluted between 15 and 17 ml together with linear chains, contrary to the CaCMC sample because

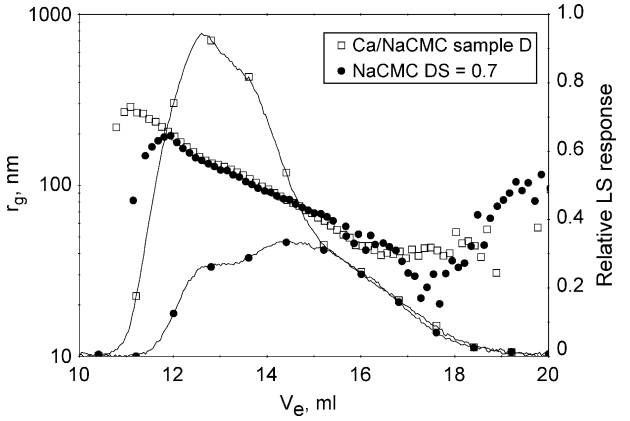

Fig. 9. The congruence of r_g vs. elution volume plots for centrifuged Ca/Na transformed CaCMC and NaCMC sample.

linear macromolecules should have the lowest mass/hydrodynamic volume ratio.

The corresponding r_g vs. elution volume plot (Fig. 9) confirms congruence also here. Log M vs. V_e plots of all CaCMC samples investigated are presented in Fig. 10. There is a small but detectable difference between pairs C, D and A, B in the middle part of molar mass interval. Otherwise all four samples appear to be very similar.

An example of non-linear conformation plots is presented in Fig. 11 for Ca/NaCMC sample A in comparison with an NaCMC sample having DS = 0.7. The exponent of a straight line fit of a conformation plot of Ca/NaCMC sample A in terms of log r_g against log M (M_w in our case) would be 0.27 and may be compared to the value 0.41 obtainable for NaCMC sample having DS = 0.7. Recently, the exponent of a straight line fit of a conformation plot of NaCMC in terms of log r_g against log M was reported to be 0.22, i.e. below hard sphere value 0.33 (Schulz, Burchard, & Dönges, 1998). Actually, an initial slope close to 0.5 in Fig. 11 indicates mainly linear coils. Above $M \sim 10^7$, an almost linear part having slope around 0.45 is observed and might be discussed as an evidence of the absence of linear coils in

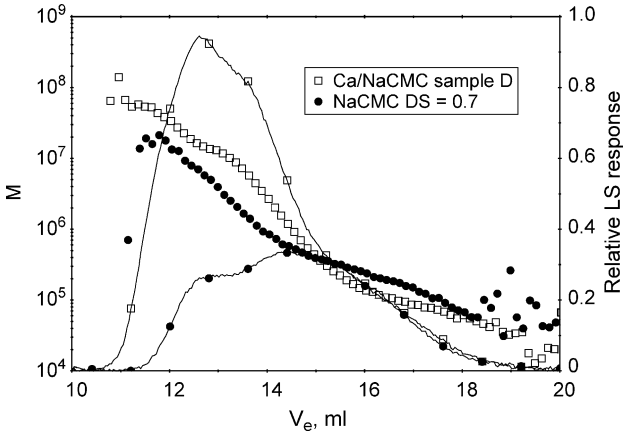

Fig. 8. The comparison of M vs. elution volume plots of centrifuged Ca/Na transformed CaCMC and NaCMC sample.

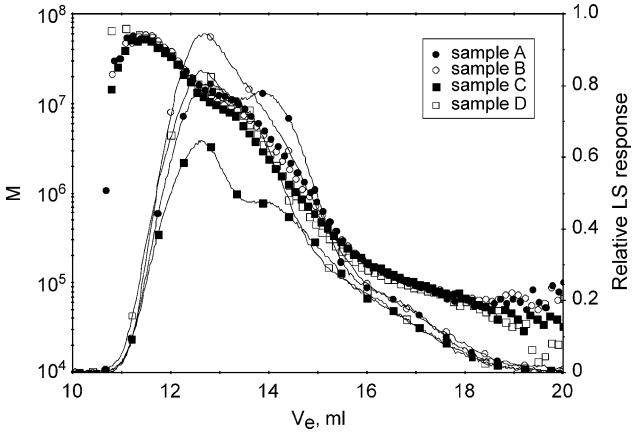

Fig. 10. The comparison of M vs. elution volume plots of centrifuged Ca/Na transformed CaCMC samples investigated.

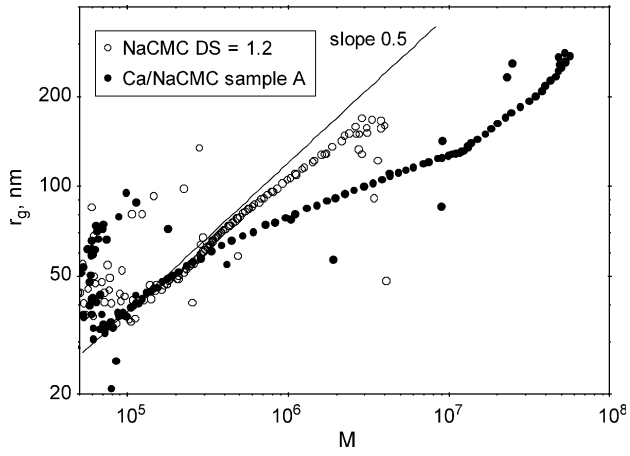

Fig. 11. Comparison of conformation plots of Ca/Na transformed CaCMC sample A and NaCMC sample having DS = 1.2.

this molar mass interval. The curvature simply reflects changes in composition of a mixture of linear and aggregated structures having the same size and no conclusions about a very dense particle structure can be drawn. The less pronounced curvature of the conformation plot obtained for NaCMC samples (Fig. 11) is related to a lower amount of fringed micelles present in these samples. Very similar non-linear plots with decreasing slope were obtained also for samples B, C, and D.

Size distributions of all CaCMC samples are displayed in Fig. 12. The linear column behavior in terms of size allowed extension of the distributions below 20 nm also here. Some difference is found only for A and B samples; the other two are almost identical. Significant differences were found in their mass recovery values. All of them were rather low ranging from 53 to 67%. This is not surprising if their low degree of substitution is taken into account. The solutions before centrifugation were slightly hazy indicating the presence of macrogels.

Preliminary filtration tests have shown that a prefiltration with a filter size 5 μm was needed to obtain good

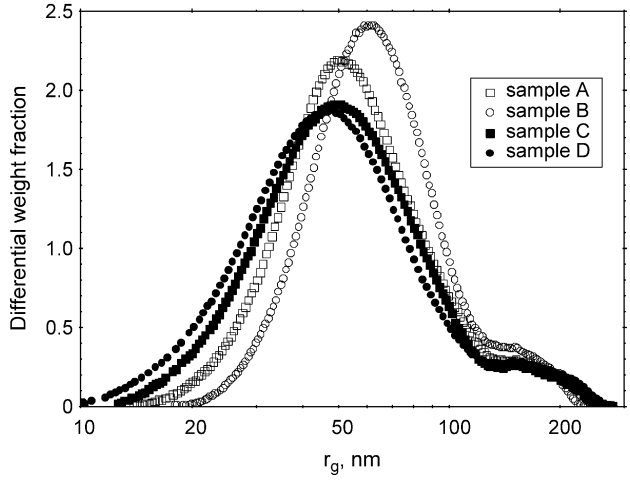

Fig. 12. Size distributions of Ca/Na transformed CaCMC samples investigated.

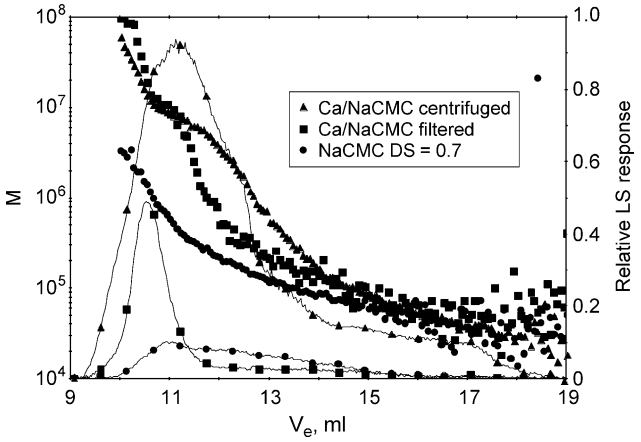

Fig. 13. Molar mass vs. elution volume plots of Ca/Na transformed CaCMC sample B after 2 μm filtration and centrifugation compared with NaCMC (DS = 0.7) filtered by 0.45 μm filter obtained using TSK column.

consecutive filterability through a set of filters described in Section 2. To avoid the danger of blockage and/or loss of the sample in the Labio column set (having particle size 10 and 5 μm stainless steel sieves), TSK 5000PW column was used because its larger particle size (17 μm) and frit porosity (10 μm) should decrease the danger of plugging and make it more tolerant to the presence of large aggregates. As the main aim of these filtration experiments was to perform something like 'sieve' analysis in terms of M_w and recovery, the use of this column, which has, according to the supplier, an exclusion limit in terms of M around 1×10^6 for poly(ethylene oxide), was acceptable. Using a broad poly(ethylene oxide), this exclusion limit was found to be about 10.7 ml under the conditions used. The log M vs. V_e plots obtained on TSK column for 2 μm filtered and centrifuged Ca/NaCMC transformed sample B are displayed in Fig. 13 together with the respective plot for NaCMC sample filtered with an 0.45 μm filter as an example. There is a large difference between filtered and centrifuged Ca/NaCMC sample in the middle part of the curves indicating a significant loss of mass during filtration which was not observed for the NaCMC reference sample (cf. Fig. 1). Accordingly, the recovery values for centrifuged and filtered Ca/NaCMC sample were obtained 67 and 19%, respectively. Also, it follows from a comparison with NaCMC reference sample (shown above to contain essentially linear coils up to M around 500 000) that

Table 1
SEC results obtained for Ca/NaCMC sample B (4.48% Ca, DS 0.59)

Sample handling	$M_w\times10^{-6}$	$M_n\times10^{-4}$	M_w/M_n	Recovery (%)
Filtration 2 μm	2.2	8.4	28	19.8
1 μm	2.1	8.7	23	20.0
0.45 μm	1.6	7.5	22	20.0
0.22 μm	0.61	7.2	8.2	19.0
Centrifugation	1.35	6.0	22	67.6

Table 2
SEC results obtained for Ca/NaCMC sample A (4.66% Ca, DS 0.62)

Sample handling	$M_w \times 10^{-6}$	$M_n \times 10^{-4}$	M_w/M_n	Recovery (%)
Filtration 2 μm	3.6	10.6	34	24.9
1 μm	3.1	8.3	38	25.0
0.45 μm	1.5	6.8	21	21.3
0.22 μm	0.21	6.3	3.3	11.6[a]
Centrifugation	1.38	5.7	24	64.7

[a] Filter plugged during second injection.

Table 4
SEC results obtained for Ca/NaCMC sample C (4.51% Ca, DS 0.60)

Sample handling	$M_w \times 10^{-6}$	$M_n \times 10^{-4}$	M_w/M_n	Recovery (%)
Filtration 2 μm	5.6	17.4	32	16.6
1 μm	5.1	13.0	40	16.7
0.45 μm	4.8	13.1	37	16.0
0.22 μm	1.2	9.3	13	11.9[a]
Centrifugation	1.43	7.8	18	53.0

[a] Second injection.

the amount of linear macromolecules in CaCMC samples decreases considerably. Let us note that the recovery values for model NaCMC samples were always higher than 90%. The SEC results obtained for the all investigated CaCMC samples after filtration and centrifugation are compared in terms of M_w, apparent values of M_n and M_w/M_n (see above) and recovery values in Tables 1–4. All samples were prefiltered using 5 μm filters because direct use of smaller filter sizes resulted in a fast filter blockage even at low filtration rates. On the other hand, several ml of all 5 μm prefiltered samples could be filtered with any of filters having pore size between 2 and 0.45 μm indicating that the macrogels removed are larger than 5 μm and the main part of filterable aggregates smaller than 0.45 μm. This is corroborated by the values of M_w and recovery in Tables 1–4. A more pronounced decrease of recovery (with the exception of sample B), related to this population of aggregates (single fringed micelles), is found only after filtration through an 0.22 μm filter.

A great decrease in the recovery after filtration compared with centrifugation should be simply related to the filtration cake effect which should be somewhat selective to non-linear structures (cf. Fig. 12). This appears to be a serious drawback of the filter use in SEC analysis of these samples because the filtered solution then represents only a minor part of the whole sample (Saake et al., 2000). Centrifugation appears to be the technique of choice here. A similar grouping as indicated in Figs. 10 and 11 follows also from Tables 1–4. The recoveries of samples A and B are higher compared with samples C and D after both filtration and centrifugation. Otherwise, all samples seem to be quite similar. This is not so surprising because their degree of substitution as one of decisive parameters of their morphology is practically the same and all four samples were selected for the same application. When looking for a criterion of batch-to-batch reproducibility, agreement of their Ca content, M_w values, recoveries after centrifugation and a match of log M vs. elution volume plots and their deviations from linearity should be sufficient, provided that a linear column set is used.

Table 3
SEC results obtained for Ca/NaCMC sample D (4.52% Ca, DS 0.60)

Sample handling	$M_w \times 10^{-6}$	$M_n \times 10^{-4}$	M_w/M_n	Recovery (%)
Filtration 2 μm	3.2	9.9	32	13.5
1 μm	2.5	10.9	23	13.9
0.45 μm	1.9	7.4	26	12.0
0.22 μm	0.45	8.6	5.6	11.8[a]
Centrifugation	1.84	6.4	28	59.0

[a] Significant decrease of recovery after second injection.

Acknowledgements

Our thank are due to Mrs M. Plichtová for AAS determinations. B.P. wishes to thank the AstraZeneca R&D Mölndal and the Academy of Sciences of the Czech Republic (project No. AVOZ 4050913) for financial support.

References

Dautzenberg, H., Lukanoff, B., & Hicke, H.-G. (1990). Charakterisierung von Cellulosederivaten durch Löslichkeituntersuchungen. *Acta Polymer*, *41*, 233–243.

Doelker, E. (1993). Cellulose derivatives. *Advances in Polymer Science*, *107*, 199–265.

Flory, P. J., & Fox, T. G., Jr. (1951). Treatment of intrinsic viscosities. *Journal of American Chemical Society*, *73*, 1904–1908.

Gruber, E. (1979). Übermolekulare Strukturen in Cellulose-Lösungen. *Papier*, *33*, 534–540.

Ioan, C. E., Aberle, T., & Burchard, W. (2001). Structure properties of dextran 3. Shrinking factors of individual clusters. *Macromolecules*, *34*, 3765–3771.

Just, E. K., & Majewicz, T. G. (1985). Cellulose ethers. In H. F. Mark, N. M. Bikales, Ch. G. Overberger, G. Menges, & J. I. Kroschwitz (Eds.), *Encyclopedia of polymer science and engineering* (Vol. 3) (pp. 226–229). New York: Wiley.

Picton, L., Merle, L., & Muller, G. (1996). Solution behavior of hydrophobically associating cellulosic derivatives. *International Journal of Polymer Analysis and Characterization*, *2*, 103–113.

Potschka, M. (1987). Universal calibration of gel permeation chromatography and determination of molecular shape in solution. *Analytical Biochemistry*, *162*, 47–64.

Potschka, M. (1988). Size-exclusion chromatography of polyelectrolytes: Experimental evidence for a general mechanism. *Journal of Chromatography*, *441*, 239–260.

Potschka, M. (1991). Size exclusion chromatography of DNA and viruses: Properties of spherical and asymmetric molecules in porous networks. *Macromolecules*, *24*, 5023–5039.

Saake, B., Horner, S., Kruse, Th., Puls, J., Liebert, T., & Heinze, Th. (2000). Detailed investigation on the molecular structure of carboxymethyl cellulose with unusual substitution pattern by means of enzyme-supported catalysis. *Macromolecular Chemistry and Physics*, *201*, 1996–2002.

Samuelson, O. (1963). *Ion exchange separations in analytical chemistry*. New York: Wiley.

Schulz, L., & Burchard, W. (1993). Lösungsstruktur verschiedener Cellulose-Derivate. *Papier*, *47*, 1–9.

Schulz, L., Burchard, W., & Dönges, R. (1998). Evidence of supramolecular structures of cellulose derivatives in solution. In T. J. Heinze, & W. G. Glasser (Eds.), *Cellulose derivatives. Modification, characterization and nanostructures*. *ACS symposium series 688* (pp. 218–238). Washington: Oxford University Press (Chapter 16).

Schulz, L., Seger, B., & Burchard, W. (2000). Structures of cellulose in solution. *Macromolecular Chemistry and Physics*, *201*, 2008–2022.

Radke, W. (2001). Simulation of GPC-distribution coefficients of linear and star-shaped molecules in spherical pores. *Macromolecular Theory and Simulations*, *10*, 668–675.

Reed, W. F. (1995). Data evaluation for unified multi-detector size exclusion chromatography—molar mass, viscosity and radius of gyration distributions. *Macromolecular Chemistry and Physics*, *196*, 1539–1575.

Wade, A., & Weller, P. J. (1994). *Handbook of pharmaceutical excipients* (2nd ed.). London: The Pharmaceuticals Press.

Wittgren, B., & Porsch, B. (2002). Molar mass distribution of hydroxypropyl cellulose by size exclusion chromatography with dual light scattering and refractometric detection. *Carbohydrate Polymers*, *49*, 457–469.